

MATERIALS

The Congo Caves (33.39°S, 22.21°E) comprises a 4 km system of chambers. In 1995, a 1.55 m tall stalagmite (CAN1) was collected ~750 m from the main Cave entrance (Fig. SI1). The caves are situated in limestone that is part of the Kango Supergroup, a Neoproterozoic siliciclastic-carbonate sequence that crops out between the steep southern early Palaeozoic Table Mountain Group of the mountain range to the north, and the flat semi-arid plains of the Oudtshoorn Basin to the south, which comprises a thick, coarse terrestrial siliciclastic ‘molasse’ sequence of Jurassic to Cretaceous age. Earlier work on the speleothems from the Congo Caves are reported by Talma and Vogel (1992) and Vogel and Kronfeld (1997).

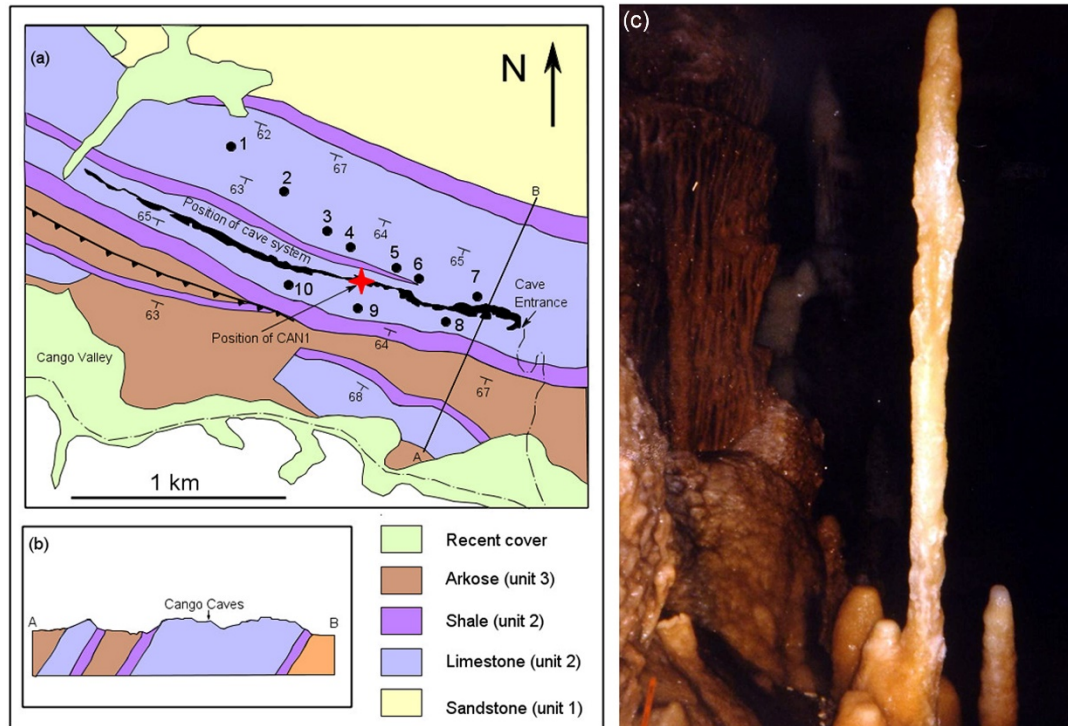


Figure SI1: Location of speleothem CAN1 in the Congo Caves system (a), regional geology (b), the CAN1 speleothem in-situ (c). Numbers = surface rock samples (SAM prefix Table SI1). Map from Doel (1995) and cave system from South African Speleological Association (1978).

Table SI1: Surface rock sample stable carbon and oxygen isotope results. Location of samples corresponds to numbers in Figure SI1.

Country rock - Matjies River Formation				
Sample		$\delta^{13}\text{C}$	$\delta^{18}\text{O}$ SMOW	$\delta^{18}\text{O}$ PDB
SAM2		0.89	24.39	-6.32
SAM3		-4.31	25.23	-5.51
SAM4		-0.69	26.23	-4.54
SAM5		2.25	27.22	-3.58
SAM7		-0.55	26.37	-4.40
SAM8		-0.61	25.60	-5.15
SAM9		1.31	26.73	-4.05
SAM10		2.71	23.47	-7.22

METHODS

CAN1 was transported to the laboratory at the University of Cape Town and cut into six pieces of equal length and then each cut in half lengthwise using a diamond tipped rotary saw. Samples for U-series dating ($n=21$, 0.2-0.36 g, Table SI2) were sent to the University of Bern, Switzerland for analysis. All analysed samples come from the central axis of the stalagmite. The carbonate in CAN1 is extremely pure and no solid residue, or cloudiness in the acid, remained after dissolution in phosphoric acid.

Samples for carbon and oxygen isotope analysis (20-25 mg each) were taken every 5 cm as close as possible to the central axis of each stalagmite and parallel to the growth rings, using a 2 mm drill bit. 110 samples of CAN1 were analysed at the University of Cape Town. The sampling of the CAN1 speleothem reflects the techniques of the day, and combined with the brittle nature of the calcite, much of the CAN1 speleothem was destroyed in the sampling process.

Samples were analysed using both off-line and standard gas-bench techniques. Off-line extraction of CO_2 from carbonates was made using the method of McCrea (1950) with 100% phosphoric acid. Samples were reacted at 25°C and a CO_2 -calcite fractionation factor of 1.01025 was used to correct the raw data. C and O isotope ratios were measured using either a Finnegan MAT252 or a Thermo XP mass spectrometer. An internal calcite standard (NM; $\delta^{13}\text{C} = 1.57\text{‰}$, $\delta^{18}\text{O} = 25.10\text{‰}$ relative to PDB and SMOW, respectively) calibrated using NBS-19 was used to normalize raw data to the SMOW and PDB scales. Repeat analysis of the NM standard suggests that the precision is 0.2 and 0.1‰ for $\delta^{18}\text{O}$ and $\delta^{13}\text{C}$, respectively. Samples were reacted at 70°C using the on-line gas bench analysed along with the standards Lincoln Limestone, NBS18 and NBS20, which have a range of $\delta^{13}\text{C}$ and $\delta^{18}\text{O}$ values. The measured and accepted values were used to construct a calibration curve and this was used to correct the raw data, and to determine the precision of the method. Repeated analyses of the standards suggest that the $\delta^{13}\text{C}$ and $\delta^{18}\text{O}$ values are accurate to within 0.14‰ and 0.18‰ (2σ), respectively.

RESULTS

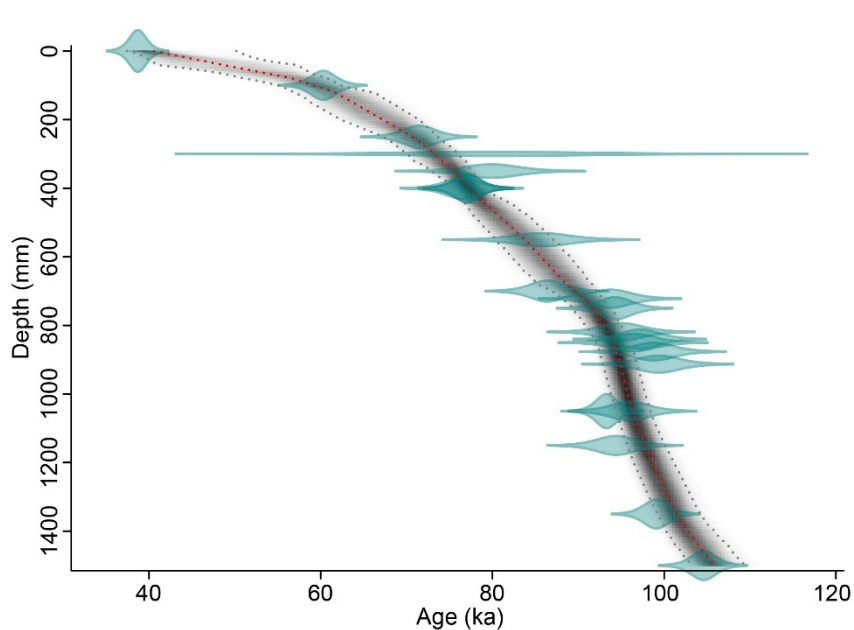
Uranium-series dating and age model development

Table. SI2: Cango Caves speleothem U-series dating results. Activity ratios calculated using the decay constants for ^{234}U and ^{230}Th determined by Cheng et al. (2013). Values/yr: ^{234}U (2.8222 ± 0.0030)E-6 and ^{230}Th (9.1706 ± 0.01335)E-6. For samples with significant Th/U ratios (Table B), corrections applied in Table A are based on the assumption that the "detrital fraction" has a Th/U ratio similar to that of average continental crust (4.2) and has U-series nuclides in secular equilibrium. Detrital fractions rarely have Th/U ratios lower than 4.2, and these corrections are the maximum to be expected.

TABLE A				Activity ratios									
Sample name	Dist, mm	ppb U	ppb Th	($^{230}\text{Th}/^{238}\text{U}$)	± 1SE	($^{234}\text{U}/^{238}\text{U}$)	± 1SE	($^{230}\text{Th}/^{234}\text{U}$)	± 1SE	App. Age (ka)	± 95%	($^{234}\text{U}/^{238}\text{U}$) init.	± 95%
CAN 1- 1	0	68.7	7.4	1.174	0.001	3.006	0.015	0.391	0.003	38.7	0.9	3.24	0.03
CAN 1- 3	100	76.8	2.6	1.389	0.001	3.097	0.005	0.448	0.004	60.3	1.3	3.49	0.02
CAN 1- 6 R	250	40.6	0.8	1.351	0.002	2.640	0.009	0.512	0.004	71.5	1.7	3.01	0.02
CAN 1- 7	300	44.0	3.4	1.474	0.009	2.654	0.006	0.556	0.024	80.3	9.3	3.08	0.06
CAN 1- 8	350	36.2	2.3	1.489	0.003	2.688	0.006	0.554	0.007	79.9	2.8	3.12	0.02
CAN 1- 9 R	400	39.5	0.5	1.516	0.002	2.814	0.007	0.539	0.005	76.5	1.8	3.25	0.02
K 9	400	48.5	n.d	1.453	0.005	2.697	0.006	0.539	0.003	77.0	1.4	3.11	0.01
CAN 1- 12	550	27.3	0.3	1.572	0.003	2.692	0.016	0.584	0.007	85.8	2.9	3.16	0.04
CAN 1- 15 R	700	54.6	0.2	1.560	0.002	2.661	0.007	0.586	0.005	86.4	1.8	3.12	0.02
CAN 1-15 B	722	55.3	10.0	1.688	0.012	2.715	0.007	0.622	0.005	93.8	2.1	3.23	0.02
CAN 1-16	750	56.3	4.4	1.685	0.012	2.700	0.004	0.624	0.004	94.3	1.7	3.22	0.02
CAN 1-17 B	819	42.7	0.5	1.709	0.012	2.717	0.011	0.629	0.005	95.1	2.2	3.25	0.03
CAN 1-17 D	840	50.0	0.8	1.744	0.012	2.727	0.003	0.639	0.004	97.2	2.0	3.27	0.02
CAN 1-18	850	59.6	1.2	1.698	0.013	2.671	0.005	0.636	0.005	96.5	2.2	3.20	0.02
CAN 1-18 B	876.5	58.4	1.0	1.709	0.012	2.650	0.006	0.645	0.005	98.8	2.2	3.18	0.02
CAN 1-19 A	913	53.0	0.9	1.785	0.013	2.751	0.005	0.649	0.005	99.4	2.2	3.32	0.02
CAN 1- 22 R	1050	56.7	0.6	1.726	0.002	2.727	0.005	0.633	0.005	96.0	2.0	3.27	0.02
K 22	1050	62.1	n.d.	1.600	0.005	2.583	0.006	0.620	0.003	93.3	1.1	3.06	0.01
CAN 1- 24 R	1150	71.3	0.1	1.727	0.002	2.765	0.004	0.625	0.005	94.4	2.0	3.30	0.02
K 28	1350	59.1	n.d.	1.746	0.006	2.698	0.008	0.647	0.004	99.1	1.3	3.25	0.02
K 31	1500	67.2	n.d.	1.821	0.006	2.712	0.007	0.671	0.004	104.6	1.3	3.30	0.01

Table. SI2 cont'd: Congo Caves speleothem U-series dating results. Activity ratios calculated using the decay constants for ^{234}U and ^{230}Th determined by Cheng et al. (2013). Values/yr: ^{234}U (2.8222 ± 0.0030)E-6 and ^{230}Th (9.1706 ± 0.01335)E-6. For samples with significant Th/U ratios (Table B), corrections applied in Table A are based on the assumption that the "detrital fraction" has a Th/U ratio similar to that of average continental crust (4.2) and has U-series nuclides in secular equilibrium. Detrital fractions rarely have Th/U ratios lower than 4.2, and these corrections are the maximum to be expected.

TABLE B				atomic		Activity ratios			
Sample name	Dist, mm	ppb U	ppb Th	$^{232}\text{Th}/^{238}\text{U}$	^{238}U Fr detrital	$(^{230}\text{Th}/^{238}\text{U})$	$\pm 1\text{SE}$	$(^{234}\text{U}/^{238}\text{U})$	$\pm 1\text{SE}$
CAN 1- 1	0	68.7	7.4	0.111	0.0278	1.169	0.001	2.950	0.015
CAN 1-3	100	76.8	2.6	0.034	0.0086	1.385	0.001	3.079	0.005
CAN 1- 7	300	44.0	3.4	0.079	0.0197	1.465	0.009	2.621	0.006
CAN 1-8	350	36.2	2.3	0.066	0.0164	1.481	0.003	2.660	0.006
CAN 1-15 B	722	55.3	10.0	0.187	0.0466	1.656	0.012	2.635	0.007
CAN 1-16	750	56.3	4.4	0.082	0.0204	1.671	0.012	2.665	0.004



U/Th ages (Table SI2) from CAN1 ranged from 38.7 ± 0.9 ka (0 mm) to 104.6 ± 1.3 ka (at 1500 mm). Some age reversals do exist, and a Bayesian technique (rbacon v.2.4.3; Blaauw and Christen, 2011) was used to create an age model that incorporated all of the available data (Fig. SI2).

Figure. SI2: Speleothem CAN1 age-depth model, established using rbacon v.2.4.3 (Blaauw and Christen, 2011).

Isotopic equilibrium

The $\delta^{18}\text{O}$ values of authigenic carbonate depend on the temperature of precipitation in the cave and the $\delta^{18}\text{O}$ value of the water from which the calcite precipitates. It is also important that isotope equilibrium be maintained. In cases where the correlation between $\delta^{13}\text{C}$ and $\delta^{18}\text{O}$ values is significant, it is probably due to kinetic effects related to evaporation, and there is limited relationship between temperature and $\delta^{18}\text{O}$ value. This situation is typical in carbonate taken from the flanks of speleothems (Hendy, 1971). For CAN1, there is no correlation between $\delta^{13}\text{C}$ and $\delta^{18}\text{O}$ values (Fig. SI3), which is consistent with precipitation of calcite in isotopic equilibrium.

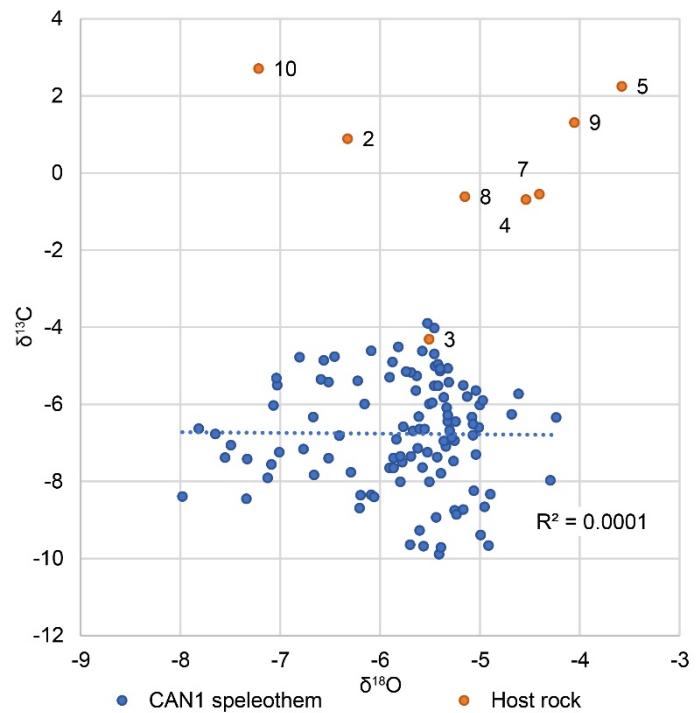


Figure. SI3: Speleothem CAN1 calcite and host rock $\delta^{13}\text{C}$ and $\delta^{18}\text{O}$ values. Lack of correlation between CAN1 $\delta^{13}\text{C}$ and $\delta^{18}\text{O}$ indicates the calcite precipitated in isotopic equilibrium.

The $\delta^{13}\text{C}$ and $\delta^{18}\text{O}$ values and composite model development

The $\delta^{13}\text{C}$ values of the samples ($n=112$) vary between -3.9‰ and -9.89‰ , and the $\delta^{18}\text{O}$ between -4.24‰ and -7.98‰ relative to the Vienna PeeDee Belemnite (VPDB) standard (Fig SI4). Kinetic fractionation during crystallization of calcite leads to strong correlation between $\delta^{13}\text{C}$ and $\delta^{18}\text{O}$ values, and it is clear that no such correlation exists (Fig SI3). Whereas the $\delta^{13}\text{C}$ values from CAN1 exhibit a high signal-to-noise ratio, the $\delta^{18}\text{O}$ values are more variable, and were smoothed using a 3-point moving average to reduce noise.

To maximise the utility of the CAN1 data and their integration into the aggregate regional dataset, the data were used as the basis for the creation of composite records integrating comparable data from Efflux Cave (Braun et al., 2020), previously published data from the Cango Caves (Talma and Vogel, 1992) and, in the case of the $\delta^{13}\text{C}$ data, data from the Seweweekspoort rock hyrax middens (Chase et al., 2017). The composite records (referred to hereafter as Cape Fold Composites; CFC) were created to obtain a coherent signal from the aggregated data (Fig. SI5, 6).

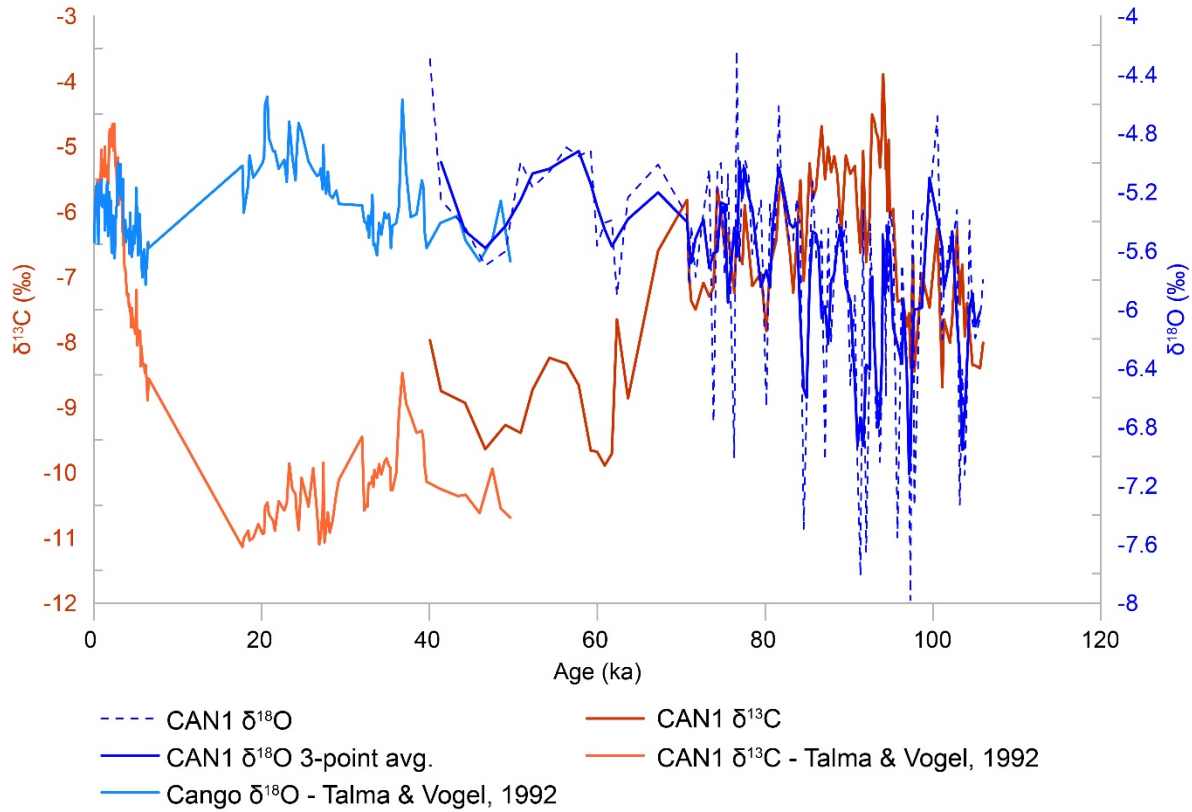


Figure. SI4: Oxygen and carbon isotope records from the Congo Caves, including the CAN1 data presented in this paper and the data of Talma and Vogel (1992).

The speleothem $\delta^{13}\text{C}$ records reflect changes in the vegetation specific to each site/record, including the potential presence of micro-scale vegetation mosaics that may result in significant differences in the $\delta^{13}\text{C}$ content of individual speleothems from the same cave, as is the case in Efflux Cave (Braun et al., 2020). It is important to note that while individual speleothem $\delta^{13}\text{C}$ contents may differ, and the amplitudes of the signals expressed may vary (both as a function of the vegetation present in the drip water source locale), the sign of the signal – reflecting the changes in climate that drive vegetation response – is generally consistent between the records considered here, indicating that a climate signal can be derived from the data. To accurately define this signal at the regional scale, it is necessary to apply scaling transformations to individual records. The Congo Caves speleothems indicate similar $\delta^{13}\text{C}$ values and amplitudes, and, based on the difference of the mean values of the overlapping portions, a simple $x-1.1968$ transformation was applied to the CAN1 $\delta^{13}\text{C}$ record to align it with the Congo Caves speleothem $\delta^{13}\text{C}$ record of Talma and Vogel (1992), creating a Congo Caves composite $\delta^{13}\text{C}$ record. To account for regional differences in vegetation composition, and render the Efflux Cave $\delta^{13}\text{C}$ records comparable both with each other and with the Congo Caves composite record, reduced major axis regression (RMA) was used between each of the Efflux Cave speleothem $\delta^{13}\text{C}$ records and the overlapping section of the Congo Caves composite $\delta^{13}\text{C}$ record to estimate scaling transformations to minimize the Euclidean distance between the datasets (for speleothem 142843, $(x*0.39647)-6.9412$; for speleothem 142848, $(x*1.354)-4.9988$; speleothems 142847 and 142849 were combined prior to scaling to improve overlap with Congo Caves composite, $(x*0.74706)-4.1018$; speleothem 142846 does not overlap with

any other record, but based on similarities in value and amplitude of variability with speleothems 142847 and 142849 the same $(x*0.74706)-4.1018$ transform was applied). Based on the similarities between the Congo Caves speleothem $\delta^{13}\text{C}$ record of Talma and Vogel (1992) and the Seweweekspoort rock hyrax midden $\delta^{13}\text{C}$ record (Chase et al., 2017), we have used this latter record to span the hiatus present in the Talma and Vogel record. As with the Efflux Cave data, RMA regression between the Seweweekspoort $\delta^{13}\text{C}$ record and the Congo Caves composite $\delta^{13}\text{C}$ record was used to estimate a scaling transformation $((x*1.642)+33.94)$ for the Seweweekspoort data. Finally, the Congo Caves, Efflux Cave and Seweweekspoort records were compiled, sorted by age, normalized using a standard score (to avoid confusion regarding reporting of corrected $\delta^{13}\text{C}$ data) and, to improve the signal to noise ratio (Fig. SI5).

The speleothem $\delta^{18}\text{O}$ records were combined to create a composite record using the same process that was applied to the $\delta^{13}\text{C}$ records, with the same goal of obtaining a record that reflects regional changes in climate with a high signal to noise ratio. As the CAN1 $\delta^{18}\text{O}$ record expresses particularly high frequency variability prior to ~70 ka (likely a product of the increase in tropical influence described in the main text) a 3-point moving average was applied as an initial step to improve the signal to noise ratio. The CAN1 speleothem and that analysed by Talma and Vogel (1992) indicate similar $\delta^{18}\text{O}$ values and amplitudes for the 40-50 ka period during which they overlap, and the records were simply compiled and sorted by age and normalized using a standard score to obtain a composite record. Determined by similarities in terms of values and amplitudes of variability between Efflux Cave speleothem $\delta^{18}\text{O}$ records 142843, 142846, 142847 and 142849 were compiled and sorted by age, to create a partial composite. The $\delta^{18}\text{O}$ record from speleothem 142848 exhibits a pattern of overall variability similar to the other Efflux Cave $\delta^{18}\text{O}$ records, but at slightly higher values and reduced amplitude of variability. RMA regression was used to estimate a scaling transformation $((x*2.3855)+4.9234)$ to minimize the Euclidean distance between the 142848 $\delta^{18}\text{O}$ record and the Efflux Cave partial composite. With this transformation applied, the 142848 $\delta^{18}\text{O}$ record was compiled with the other Efflux Cave $\delta^{18}\text{O}$ records, and the aggregate was sorted by age and normalized using a standard score. RMA regression was then applied to the overlapping sections of the Congo Caves and Efflux Cave composite $\delta^{18}\text{O}$ records, with a scaling transform of $(x*0.61024)+0.16217$ being applied to the Efflux Cave composite to create a coherent regional CFC composite $\delta^{18}\text{O}$ record (Fig. SI6).

Both the CFC $\delta^{13}\text{C}$ and $\delta^{18}\text{O}$ records were smoothed using a Gaussian kernel method with a kernel width $\sigma = 0.3$ ka. These composites are plotted with 95% confidence intervals for the reconstructions in Fig. SI5,6. Uncertainties associated with age estimates are indicated in Table SI2 and the original papers describing the Efflux Cave speleothems (Braun et al., 2020) and the speleothem from the Congo Caves analysed by Talma and Vogel (1992; Vogel and Kronfeld, 1997).

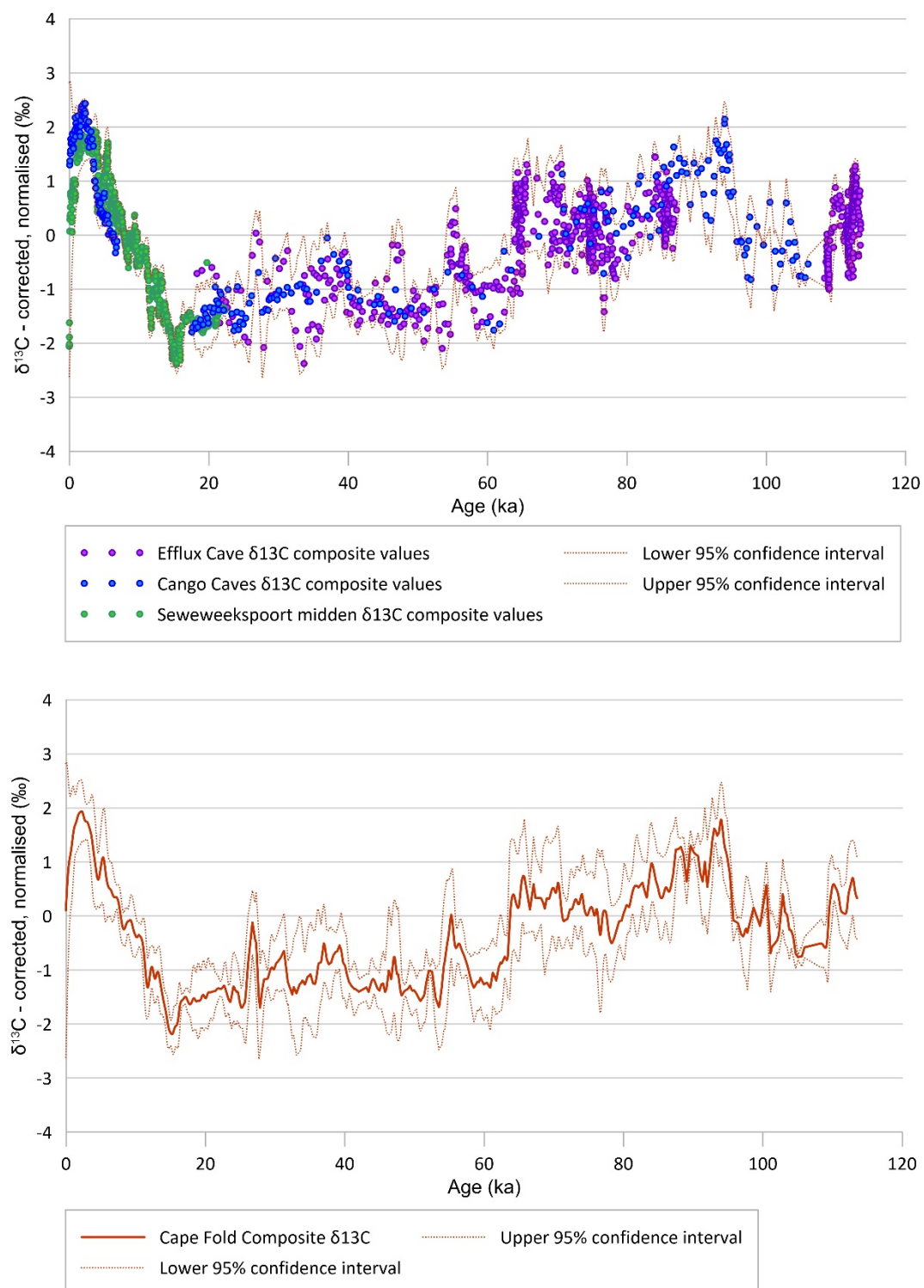


Figure. SI5: Cape Fold Composite $\delta^{13}\text{C}$ record: Component and composite stable carbon isotope records from the Cango Caves - CAN1 and the data of Talma and Vogel (1992), Efflux Cave (Bar-Matthews et al., 2010; Braun et al., 2020), and the Seweweekspoort rock hyrax middens (Chase et al., 2017). Composite records and 95% confidence intervals for the composite were established using a Gaussian kernel method with a kernel width $\sigma = 0.3$ ka.

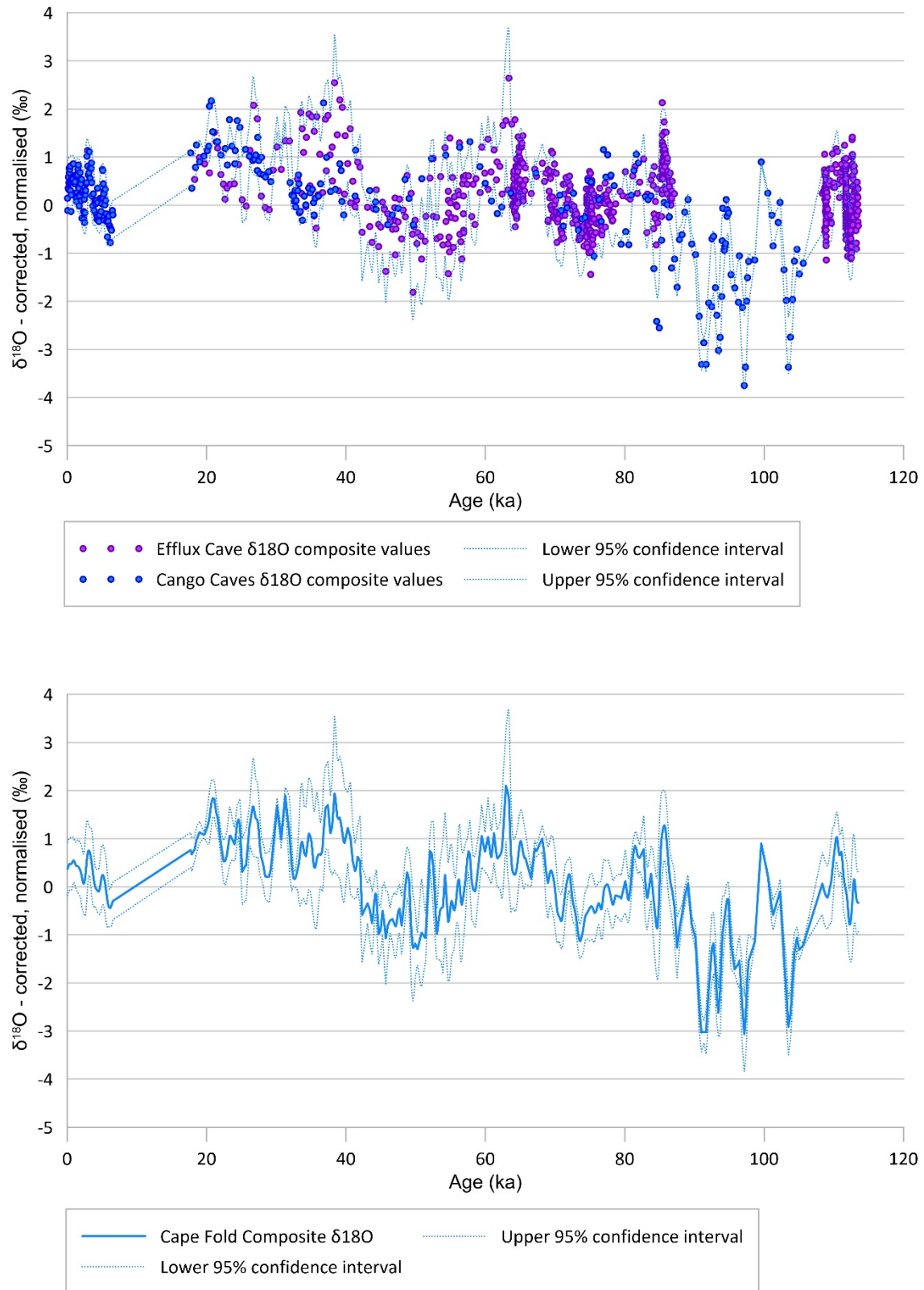


Figure. SI6: Cape Fold Composite $\delta^{18}\text{O}$ record: Component and composite stable oxygen isotope records from the Cango Caves - CAN1 and the data of Talma and Vogel (1992) - and Efflux Cave (Bar-Matthews et al., 2010; Braun et al., 2020). Composite records and 95% confidence intervals for the composite were established using a Gaussian kernel method with a kernel width $\sigma = 0.3$ ka.

REFERENCES

- South African Spelaeological Association, 1978, *Cango Cave - The combined 1956 & 1978 surveys by the S.A. Spelaeological Association (Cape Section)*.
- Bar-Matthews, M., Marean, C. W., Jacobs, Z., Karkanas, P., Fisher, E. C., Herries, A. I. R., Brown, K., Williams, H. M., Bernatchez, J., Ayalon, A., and Nilssen, P. J., 2010, A high resolution and continuous isotopic speleothem record of paleoclimate and paleoenvironment from 90 to 53 ka from Pinnacle Point on the south coast of South Africa: *Quaternary Science Reviews*, v. 29, no. 17-18, p. 2131-2145.
- Blaauw, M., and Christen, J. A., 2011, Flexible paleoclimate age-depth models using an autoregressive gamma process: *Bayesian Analysis*, v. 6, no. 3, p. 457-474.
- Braun, K., Bar-Matthews, M., Matthews, A., Ayalon, A., Zilberman, T., Cowling, R. M., Fisher, E. C., Herries, A. I. R., Brink, J. S., and Marean, C. W., 2020, Comparison of climate and environment on the edge of the Palaeo-Agulhas Plain to the Little Karoo (South Africa) in Marine Isotope Stages 5–3 as indicated by speleothems: *Quaternary Science Reviews*, v. 235, p. 105803.
- Chase, B. M., Chevalier, M., Boom, A., and Carr, A. S., 2017, The dynamic relationship between temperate and tropical circulation systems across South Africa since the last glacial maximum: *Quaternary Science Reviews*, v. 174, p. 54-62.
- Cheng, H., Lawrence Edwards, R., Shen, C.-C., Polyak, V. J., Asmerom, Y., Woodhead, J., Hellstrom, J., Wang, Y., Kong, X., Spötl, C., Wang, X., and Calvin Alexander, E., 2013, Improvements in ^{230}Th dating, ^{230}Th and ^{234}U half-life values, and U–Th isotopic measurements by multi-collector inductively coupled plasma mass spectrometry: *Earth and Planetary Science Letters*, v. 371-372, p. 82-91.
- Doel, S. L., 1995, *Cango Caves stable isotope stratigraphy* [BSc Honours: University of Cape Town].
- Hendy, C. H., 1971, The isotopic geochemistry of speleothems--I. The calculation of the effects of different modes of formation on the isotopic composition of speleothems and their applicability as palaeoclimatic indicators: *Geochimica et Cosmochimica Acta*, v. 35, no. 8, p. 801-824.
- Talma, A. S., and Vogel, J. C., 1992, Late Quaternary paleotemperatures derived from a speleothem from Cango Caves, Cape Province, South Africa: *Quaternary Research*, v. 37, no. 2, p. 203-213.
- Vogel, J. C., and Kronfeld, J., 1997, Calibration of radiocarbon dates for the Late Pleistocene using U/Th dates on stalagmites: *Radiocarbon*, v. 39, no. 1, p. 27-32.